Fracture Mechanics of Concrete Structures, de Borst et al (eds) © 2001 Swets & Zeitlinger, Lisse, ISBN 90 2651 825 0

Simulation strategies for RC buildings under seismic loading

T.S.Han, S.L.Billington & A.R.Ingraffea
School of Civil and Environmental Engineering, Cornell University, Ithaca, NY, U.S.A.

ABSTRACT: Seismic analyses of reinforced concrete frame structures are performed using the finite element method to identify and propose efficient modeling strategies for the development of fragility information for frame structures. For efficient analysis, an approach of concentrating nonlinearity into possible failure sections while other portions of the simulation model remain elastic is suggested. The method is applied to a frame structure by inserting cohesive interface elements at failure sections and calibrating the constitutive model for the interface elements. Two shake table tests of a lightly reinforced concrete 3-story frame building are simulated to investigate the accuracy and efficiency of the suggested modeling strategy for the reinforced concrete frame buildings.

1 INTRODUCTION

The objective of this research is to diagnose the state-of-the-art in finite element analysis for large-scale reinforced concrete structures for seismic analysis. Simulation of reinforced concrete structures is currently limited by the level of detail affordable for efficient analysis. More robust models and modeling techniques to simulate seismic behavior of structural concrete are needed.

The current effort is aimed at the development of efficient modeling strategies which can be used reliably in state-of-the-art software to develop fragility curves for new and existing structures (Shinozuka et al. 2000). To supplement the high cost of experimental methods and to generate fragility information where no earthquake data is available, data from the simulation may be used. However, it is known that performing a detailed time history analysis to capture accurate damage of reinforced concrete structures requires extensive computational efforts. Therefore, the objective of the current research is to propose and investigate efficient and reasonably accurate simulation strategies to develop fragility information using material properties and parameters (as opposed to section properties obtained from experiments).

For model calibration, a shake table experiment of a lightly reinforced concrete frame building is simulated (El-Attar et al. 1991). Different modeling approaches are investigated for the representation of reinforced concrete using this shake table test. To improve computational efficiency, a cohesive element approach is suggested and applied to the frame structure. The improvement in numerical efficiency is facilitated by concentrating nonlinearities at the failure sections while other portions of the structure remain elastic.

The calibrated interface model for the El-Attar shake table test is applied to another shake table test (Bracci et al. 1992). This test was of the same prototype structure at a different scale. The accuracy and efficiency of the cohesive element approach as a tool for developing fragility curves for frame structures are discussed.

2 COMPUTATIONAL METHODOLOGY

Two different modeling strategies are considered for the seismic analysis of the frame structure. One is a distributed nonlinearity approach, and the other is a concentrated nonlinearity approach.

A smeared cracking model is used for distributed nonlinear behavior of concrete with plane stress and frame elements (referred to as the Plane Stress Model and the Frame Model, respectively). An elasticity-based total strain rotating crack model (Fig. 1) is used for both the tensile and compressive behavior of concrete (Feenstra et al. 1998). Unloading and reloading follows a simple secant method.

An investigation of failure modes of concrete frame structures due to earthquakes reveals that most of the failures occur at the connections around joints and at the base of columns. Based on these observations, an analysis approach is proposed to improve the solution efficiency, wherein interface elements are used at the face of joint connections (Interface Model, Fig. 2).

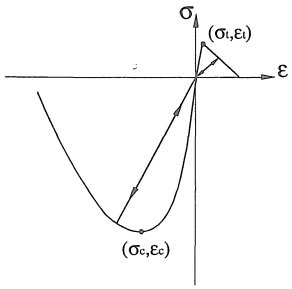

Figure 1: Total Strain Constitutive Model

The idea of this modeling approach is to concentrate the nonlinearities of the structure into these sections while the rest of the structure is modeled as elastic material (concentrated nonlinearity approach). This approach for concentrating the nonlinearities is similar to the methodology used by Rots et al. (1999) for the analysis of masonry structures. Frame elements are used for the elastic portions of the concrete. The interface elements with a nonlinear constitutive model are used to represent the concrete degradation at the failure sections.

A total-strain-based nonlinear concrete constitutive model is used for the interface element (Fig. 3). The normal-shear-mode coupled cohesive constitutive model for the interface element is based on Ortiz & Pandolfi (1999). The formulation is described in detail in Han (2001). Simple secant unloading/reloading is assumed for both tension and compression of the concrete as shown in Figure 3. The constitutive model for the interface element was implemented using a user-supplied subroutine in a commercial finite element program.

Embedded reinforcement elements are used for the reinforcing bars in the frame elements, and across the interface elements. The von Mises criterion is used for the nonlinear material model for reinforcing steel with only isotropic hardening of the steel. A bi-linear or a tri-linear relationship is used for the reinforcing steel depending on the available data from experiments. Although bondslip is not explicitly considered in the analysis, bondslip is partially accounted for through a reinforcement model parameter described next.

Since the constitutive model for the interface element uses a stress-displacement relationship, an additional geometric length scale should be provided to develop the interface constitutive model from the stress-strain relationship. The displacement axis for the interface constitutive model is scaled by multiplying the strain axis by a certain geometric quantity, in this case a length parameter. The scaling length parameter is determined by equating the energy stored in the interface element with the energy dissipated during the failure process of the frame member. The scaling length for the concrete is selected as a crack damage width in one case and as a hinge length in another

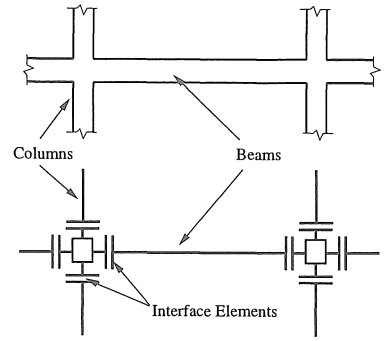

Figure 2: Use of Proposed Interface Element

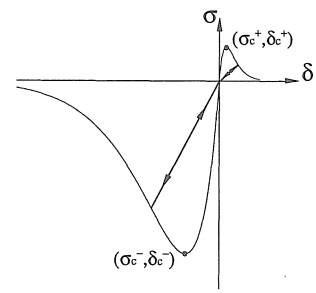

Figure 3: Cohesive Traction Separation Model

(Sec. 5.1). The scaling length for the reinforcement is selected as twice the scaling length for the concrete to consider the bondslip effect. The detailed explanation on these scaling lengths is given in Han (2001).

3 EXPERIMENT

Two shake table tests are simulated in this study. Both tests were to investigate the seismic performance of a reinforced concrete frame building designed only for gravity load. Brief descriptions of both shake table tests are given below.

3.1 *El-Attar shake table test*

The first shake table test was carried out at Cornell University (El-Attar et al. 1991). The model was a 1/8-scale lightly reinforced concrete 3-story office building. The model structure represented one bay with two side quarter bays by three bays of the prototype structure.

The total height of the structure is 1372 mm and the total width is 2057 mm in the loading direction, and 686 mm transverse to the loading direction. The column height per story is 457 mm with a cross section of 38 mm × 38 mm. The width of the beams is 34 mm, and the depth of the beams is 38 mm. The thickness of the slab is 19 mm. The base of the columns were bolted to supporting beams. The supporting beams were bolted to the shake table.

The compressive strength of the micro-concrete

was 26.2 MPa. The Young's modulus of the concrete was 13.8 GPa. The yield strength of the reinforcement was 275 MPa with a Young's modulus of 200 GPa. After the yield plateau, a strain hardening modulus of 3.46 MPa was observed after 0.03 strain. Masses in the form of lead blocks were added to the model structure to simulate the dead weight of the prototype building. The model building was subjected to a 0.18 g Taft earthquake.

3.2 *Bracci shake table test*

The other shake table test being simulated was performed at The University at Buffalo (Bracci et al. 1992). The model is a 1/3-scale reinforced concrete 3-story building designed only for gravity load. The prototype structure before scaling of El-Attar's and Bracci's Model are the same.

The model structure has the total height of 3200 mm and the total width of 5486 mm in the loading direction, and 1829 mm transverse to the loading direction. The column height per story is 1219 mm with a cross section of 102 mm × 102 mm. The width and depth of the beams are 76 mm and 102 mm, respectively, and the thickness of the slab is 51 mm.

The measured concrete compressive strength and Young's modulus from the cylinder tests is 24.1 MPa and 26.9 GPa, respectively. The tensile strength of the concrete is selected as one tenth of the concrete compressive strength. For most of the longitudinal reinforcement, the measured yield strength is 468.5 MPa. Young's modulus is 213.9 GPa, and the hardening modulus is 3.45 MPa. An ultimate stress of 503 MPa and an ultimate strain of 0.15 were obtained from tensile tests. For the upper longitudinal reinforcement in the beams of the side bays, the yield and ultimate stress is 262 MPa and 372 MPa, respectively. Young's modulus, the hardening modulus, and the failure strain are the same for both types of reinforcement. Masses in the form of lead and concrete blocks were added to the model structure to simulate the dead weight of the prototype building. The model building that was subjected to a 0.30 g Taft earthquake is simulated. More detailed description on the material properties from the experiments are given in Bracci et al. (1992).

4 FINITE ELEMENT MODEL

Three modeling approaches, a plane stress element approach, a frame element approach, and an interface element approach for modeling the concrete structure, are investigated in this study.

In Figure 4, the 2D finite element mesh for the Plane Stress Model is shown. 8-noded plane stress elements are used for the concrete. Embedded reinforcement and point masses are used for modeling reinforcement and added lead blocks, respectively. A 3×3 Gauss integration scheme is used. The connections between the column and the the shake table of the Plane Stress Model are fixed.

The 2D finite element mesh of the Frame Model is presented in Figure 5. The beams and columns consist of 3-noded Mindlin-Reissner 2D beam elements in which the stiffnesses are based on a displacement formulation. As in the plane stress approach, embedded reinforcement elements are used to model steel reinforcement, and the lead blocks are represented by point mass elements. Embedded reinforcement elements are shown above and below the frame elements in Figure 5. The stiffness of the embedded reinforcement is automatically included and updated into the frame elements during analyses. Two Gauss points are used along the beam's longitudinal axis. Six Gauss points are used along the cross section of the beam elements. This arrangement is chosen to provide sufficient flexibility in the frame elements and to prevent abrupt changes in stress at the Gauss points during material degradation. A parametric study was conducted to determine this minimal number of Gauss points to provide sufficient flexibility. The connections between the columns and the shake table are fixed for the Frame Model.

The finite element mesh for the Interface Model is shown in Figure 6. 3-noded Mindlin-Reissner 2D beam elements are used for the elastic portions of the beams and columns. The 6-noded 2D interface elements are inserted in the predicted failure sections of the columns attaching a center node of the interface element to an end of the frame element (Fig. 2). Two 4-noded 2D interface elements are used for the predicted failure sections of the beam elements each representing a different thickness in the upper and the lower portions of the T beam (beam and slab). Each end of the interface element is connected to the end of the frame element in the beams. The displacements of the end nodes of the interface elements, due to the rotation of the nodes attached to the frame element, are specified by a linear rotational relationship using constraints. A 2×6 Gauss numerical integration scheme is used for the elastic frame elements as in the Frame Model. The Lobatto numerical integration is used for the interface elements. For interface elements in columns, 10 integration points are used. For the interface elements of the upper and the lower portions of the beams, 5 and 10 integration points are used respectively. The bases of the columns in the Interface Models are fixed when the full concrete stiffness is used, and are released using rotational springs for a calibrated Interface Model (when a reduced concrete stiffness is used).

5 ANALYSIS

5.1 *El-Attar shake table test*

In the El-Attar shake table test simulation, the performance of three modeling approaches is compared. For the performance comparison, each model uses the

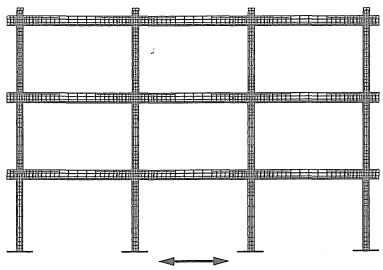

Figure 4: Plane Stress Model

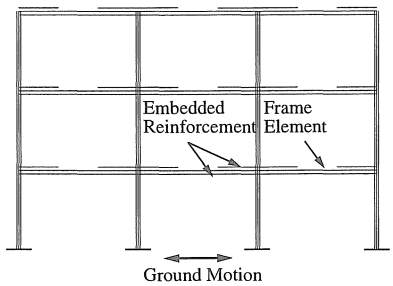

Figure 5: Frame Model

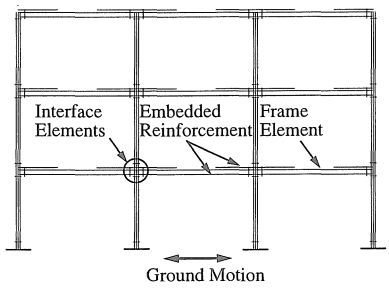

Figure 6: Interface Model

full concrete stiffness and fixed boundary conditions. Later, the seismic analysis of a calibrated Interface Model is performed.

Seismic analysis of full stiffness models

Nonlinear seismic analyses with the 0.18 g Taft earthquake are performed for the Plane Stress, the Frame, and the Interface Models and compared with experimental results. The implicit Newmark-β time integration is used, and the time step size is selected as 0.005 seconds. (The input acceleration data has a time step size of 0.01 seconds.) For the analysis convergence criteria, an energy norm of 0.1 % is used. Rayleigh damping for mass and stiffness is used, and an eigenvalue analysis is performed to determine the coefficients for the damping matrix.

For interface elements in the Interface Model, the damage lengths (scaling lengths, Sec. 2) are selected as 12.7 mm (1/3 H, where H = column or beam depth) for the concrete and 25.4 mm (2/3 H) for the reinforcing steel. The selected damage length for concrete is similar to a damage width of a single dominant crack which is about 5 times the maximum aggregate size (Bazant & Oh 1983). The additional damage length for steel is selected as half of the damage length of the concrete on each side of the hinge to consider the effects of bondslip. Thus, the total damage length for steel is selected as twice the damage length for concrete.

Eigenvalues of the Plane Stress Model, the Frame Model, and the Interface Models are compared with the experimental results. The natural frequency of three models are 15 - 25 % higher than the experimental value (Tab. 1).

The seismic analysis results of the Plane Stress Model, the Frame Model, and the Interface Model are compared with the experimental results. The calculated 3rd story displacements at the top left of all the models (Figs. 4-6) show deviation from the experiment (Fig. 7). The predicted 3rd story maximum displacements among the three models underestimate the experimental displacement by 45 % as shown in Figure 7. The displacement time history results among three models are the same during the first 3 seconds of the test when the response is dominated by the applied force or the table acceleration. However, the three simulation results deviate after 3 seconds (after the peak displacement) where the structural response is dominated by the stiffness of the structure itself. The difference in structural behavior is due to the varying stiffness reduction of the three models. It is recognized that differences between the concentrated (Interface) and distributed (Plane Stress and Frame) nonlinear approaches may also arise due to the level of detail of the modeling. Even between the distributed nonlinear approaches, the different formulation of the element might have caused some difference in response.

Table 1: Natural Frequencies

Model	Frequencies (Hz)		
	f_1	f_2	f_3
Experiment	2.20	6.10	9.55
Plane Stress Model	2.75	8.23	13.11
Frame Model	2.61	7.70	11.05
Interface Model	2.51	7.26	11.28
Interface Model (C)†	1.65	4.83	7.41

† Calibrated Model

The 1st and 2nd story displacement time histories among the models also showed similar results as the 3rd story displacement histories. No reinforcement yielding is predicted from the simulation results from all three modeling approaches. The measured moments from the experiment in some members exceeded the design moment, which implies: the reinforcement yielded in the experiment (Bracci et al. 1992).

The efficiency of each model in terms of computational time is presented in Table 2 for 12 seconds of time history analysis. The analyses are performed on a DEC Alpha workstation with 600MHz CPU and 1GB of RAM. By comparing the total time to run the 12 seconds of the time history analysis among models, the Interface Model could run the same simulation *twenty-five times faster than* the Plane Stress Model, and *twice as fast as* the Frame Model.

The Plane Stress Model has eight times as many degrees of freedom as the frame model, with six times as many Gauss points as compared to the Frame Model. The Plane Stress Model also has about eight times as many degrees of freedom as the Interface Model, but sixteen times as many Gauss points as compared to the Interface Model. Although CPU time consumption for the Plane Stress Model is only ten times and seventeen times larger than the Frame Model and the Interface Model, respectively, IO time consumption of the Plane Stress Model is twenty seven times, and eighty seven times larger than the Frame Model and the Interface Model, respectively. This suggests that a more efficient IO handling approach should be investigated to improve the efficiency of the simulation.

It is concluded that the Interface Model approach improves the computational efficiency significantly,

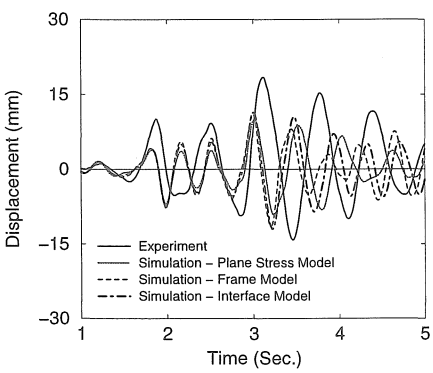

Figure 7: 3rd Story Displacement Comparison (Uncalibrated Models)

predicting similar results compared with other modeling approaches.

Seismic behavior of calibrated Interface Model

The difference between the simulation results and the experimental results is attributed to differences in the initial stiffness (higher initial natural frequency) and the level of material degradation during the earthquake. This motivates further calibration of the constitutive models to accurately simulate the experiment.

In the previous section, it is shown that the most efficient approach among the three models is the Interface Model. Additionally, further calibration of the Interface Model is less complicated than other modeling approaches since the interface element uses a stress versus relative displacement (σ vs. δ) relationship. Also, the σ vs. δ relationship is more direct for characterizing the localized degradation process compared to continuum-based constitutive relationships. Therefore, the Interface Model is further calibrated for efficient and accurate prediction of the experimental results.

Rotational spring elements are used to represent the column connections to the base and shake table. The rotational spring stiffness (1.13E+6 N-m/rad) is approximately calculated using the available drawings of the connection between the building and the shaking table. The stiffness of the concrete (EI_c) was selected as 60 % for the columns, and 50 % for the beams by reducing the Young's modulus (E). The reduction of the concrete stiffness is based on the assumption of stiffness degradation due to creep and shrinkage induced micro-cracking. Similar values have been reported and recommended by other researchers (Aycardi et al. 1992, D'Ambrisi & Filipou 1997). Since the pre-existing micro-cracking implies initial damage accumulation, it is assumed that the fracture energy of concrete is also reduced in proportion to the initial stiffness reduction.

To model the stiffness and strength degradation of the structure precisely, the shape of the constitutive model of the interface element should be extensively calibrated considering the damage evolution with a concentrated nonlinearity procedure. However, to combine with the simple geometric representation of the degradation process using interface elements, a simple calibration based on the hinge length of a frame structure is suggested for the interface constitutive model. For calibration, the damage length, similar to the size of the hinge length, is assigned to the constitutive model for the interface elements to equate the energy dissipation from the interface element with the energy dissipation from a frame member at failure. In the calibrated Interface Model, the damage lengths of 2 H (again, H = depth of member) for concrete and 4 H for steel are used (Sec. 2). An experimental investigation shows that bondslip occurs primarily in a zone between 10 - 30 times the reinforcing bar diameter (Shima et al. 1987). The increment of the steel damage length to the concrete damage length for the calibrated Interface Model is on the same order of magnitude as the primary bondslip zone length from the experimental observation. More detailed description on the stiffness calibration and interface model calibration is given in Han (2001).

Eigenvalues from the calibrated Interface Model (Interface Model (C)) and the experiment of the 3-story building are compared in Table 1. The selected constitutive model with combinations of damage length for concrete and steel predicted lower natural frequencies than ones from the experiment due

Table 2: Seismic Analysis Runtime Comparison

Model	DOFs	Gauss Points†	Iterations	CPU (Sec.)	IO (Sec.)	Total Time (Sec./Hr.)
Plane Stress	7077	9162	5307	58963	36354	95317 / 25
Frame	888	1512	3048	5930	1336	7266 / 2
Interface	930	586	2729	3369	419	3788 / 1

† Number of Gauss points in embedded reinforcements is not included.

to the lower initial stiffness of the simulation model. The initial first natural frequency of the calibrated Interface Model is 25 % lower than the experimental result.

The displacement time history results of the 3-story building of the calibrated Interface Model are shown in Figures 8-10. Time histories results during the excitation are similar between the simulation and the experiment. The maximum positive amplitude of the 3rd story displacements between the simulation and the experiment are nearly the same. However, the maximum negative amplitude of the 3rd story displacement from the simulation is 28 % larger than that of the experiment. The overall amplitudes of the simulation results are generally larger than the experimental results. The larger displacements and velocities during initial excitation predicted from the simulation are attributed to its lower initial stiffness. This most likely led to the larger initial displacements in the simulation compared to the experiment.

The magnitudes of maximum stresses in the reinforcing bars are under the elastic limit. In particular, the maximum stress at critical sections is less than 85 % of the yield stress. In terms of the damage, the simulation predicts weak column / strong beam behavior of the structure which was also observed in the experiment (Han 2001). The most damaged column from both the simulation and experiment is the 2nd column from the left in the 1st story in Figure 6. Although the detailed failure mode could not be investigated due to a lack of available experimental data, the maximum section moment at the bottom of the column from the simulation (209 N-m) is within 3 % of the experimental result (215 N-m).

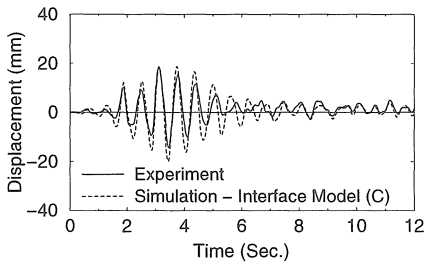

Figure 8: 3rd Story Displacement, (El-Attar's Model)

It is concluded that the calibrated Interface Model reproduced the experimental results with reasonable accuracy for the shake table test performed by El-Attar et al. (1991).

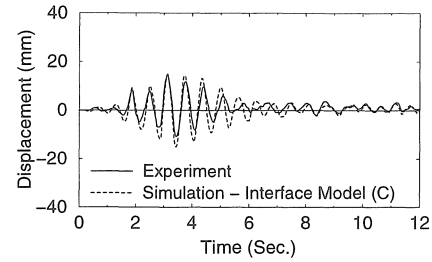

Figure 9: 2nd Story Displacement, (El-Attar's Model)

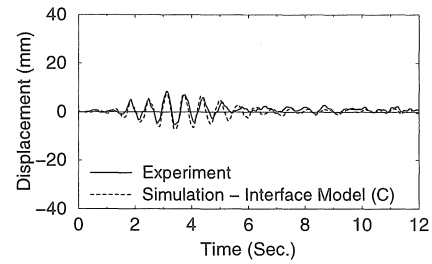

Figure 10: 1st Story Displacement, (El-Attar's Model)

5.2 *Bracci shake table test*

To confirm the possibility that the calibrated model from the El-Attar shake table test can be generally used for a seismic analysis of a frame building, a different shake table test of a frame building (Bracci et al. 1992) is simulated with the same interface model and parameter definitions (i.e. 2 H and 4 H for the concrete and steel length parameters, respectively) as used in the simulation of the El-Attar shake table test. As in the seismic analysis of the El-Attar shake table test, the first and the second modes are used to determine the Rayleigh damping coefficients with 2 % and 5 % damping for the first and the second modes.

A seismic analysis of the shake table test with a 0.30 g Taft earthquake is performed. The displacement time history results of each story of the simulation and experimental results are compared in Figures 11-13. The period of vibration from the simulation results remains in-phase with the experimental results for most of the response. Although both the positive and negative maximum 3rd story displacements from the simulation are 10 % lower than the experimental values, amplitudes of the simulation results are generally similar to the experimental results.

Similar to the El-Attar shake table test, the most damaged column member is the 2nd column from the left in the 1st story (Fig. 6) according to results

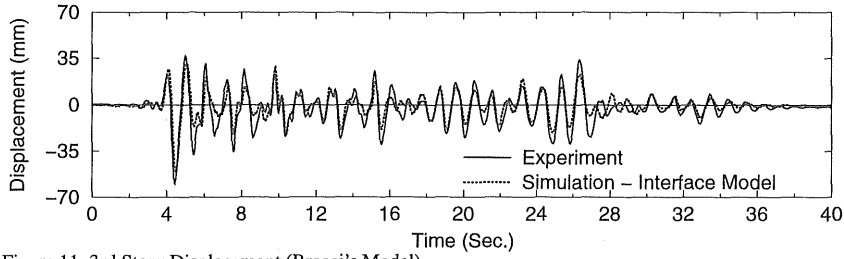

Figure 11: 3rd Story Displacement (Bracci's Model)

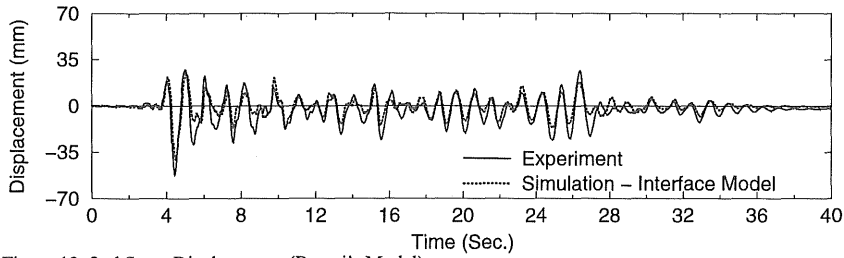

Figure 12: 2nd Story Displacement (Bracci's Model)

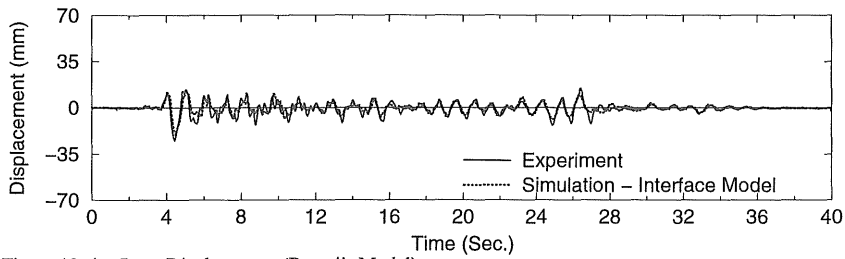

Figure 13: 1st Story Displacement (Bracci's Model)

from both the simulation and experiment. The axial force in this column in the simulation (57.9 kN) is slightly lower than the axial force from the experiment (62.3 kN). However, the maximum positive bending moment (2.5 kN-m) and maximum negative bending moment (2.3 kN-m) predicted from the simulation are 66 % and 50 % of those from the experiment, respectively. The measured positive and negative bending moment exceeded the design moment, and predicted tension-controlled failure according to the design interaction diagram. However, the simulation predicts compression-controlled failure for the positive bending moment according to a design interaction diagram based on the calibrated material parameters, and no failure in negative bending.

The maximum stress (-210.8 MPa) in the embedded reinforcement in the interface element is less than 45 % of the yield stress (468.5 MPa). The concrete crushing strain is exceeded in the outermost Gauss points in the interface element at the column. This stress distribution at the section also confirms that the simulation predicts a compressive failure of the column. Detailed descriptions of the results are given in Han (2001).

It is concluded that the Interface Model calibrated to the El-Attar shake table test predicts seismic behavior of a similar frame structure reasonably well. However, it is noted that more calibration of the cohesive model is needed to accurately predict the local behavior and failure modes of the frame structure. In addition, other frame structure experiments subjected to seismic loads should be simulated for further verification of the Interface Model approach.

6 CONCLUSION

The state-of-the-art of finite element seismic analysis of a large-scale reinforced concrete structure is investigated. Shake table tests of lightly reinforced concrete three story buildings were simulated. During the model calibration process, three modeling approaches were investigated; the Plane Stress Model, the Frame Model, and the Interface Model. All three models with the full initial concrete stiffness and fixed boundary conditions could not predict the experimental results well, although the behavior among the models was similar. The Interface Model could run the same seismic analysis with similar accuracy,

two times faster than the Frame Model and twenty-five times faster than the Plane Stress Model.

Shake table tests were further simulated with a calibrated Interface Model to improve the accuracy. Instead of a detailed constitutive model for the cohesive element, the proposed interface model has a simple constitutive model and calibration process. The simple model was selected because not only the proposed interface model has a coarse geometrical representation of the structure but also the detailed model can result in numerical divergence problems. It is concluded that the global seismic analysis results were reasonably accurate, but detailed model calibration may be needed to improved the accuracy of the local behavior and failure mode prediction of the simulation.

The current study indicates that the interface model approach may be more advantageous than the frame model approach in terms of accuracy, efficiency, and simplicity for large-scale seismic analyses of reinforced concrete frame structures. It is concluded that the Interface Model may be able to predict the global seismic behavior of reinforced concrete frame structures designed for gravity loads accurately and efficiently for moderate earthquakes. After further calibration of the simulation model, local damage prediction as well as failure modes may also be better identified. Although more rigorous constitutive model calibration may be needed to predict the local damage accurately, the proposed Interface Model gives insight into the possibilities of using simulation which could supplement experimental and field data in developing fragility curves for frame structures.

7 ACKNOWLEDGMENTS

The authors gratefully acknowledge the contributions of Dr. Peter Feenstra of the Cornell Theory Center, and Mr. Keith Kesner of Cornell University. This research was funded in part by the Multi-Disciplinary Center for Earthquake Engineering Research (MCEER), which is a National Science Foundation Engineering Education Research Center. The finite element program DIANA was used for the calculations.

REFERENCES

Aycardi, L.E., Mander, J.B. & Reinhorn, A.M. 1992. Seismic Resistance of Reinforced Concrete Frame Structures Designed Only for Gravity Loads: Part II - Experimental Performance of Subassemblages. *Technical Report NCEER-92-0028*. Buffalo: NCEER.

Bazant, Z.P. & Oh, B.H. 1983. Crack band theory for fracture of concrete. *Materials and Structures* 16(93): 155-177.

Bracci, J.M., Reinhorn, A.M. & Mander, J.B. 1992. Seismic Resistance of Reinforced Concrete Frame Structures Designed Only for Gravity Loads: Part III - Experimental Performance and Analytical Study of a Structural Model. *Technical Report NCEER-92-0029*. Buffalo: NCEER.

D'Ambrisi, A. & Filippou, F.C. 1997. Correlation studies on an RC frame shaking-table specimen. *Earthquake Engineering and Structural Dynamics* 26: 1021-1040.

El-Attar, A.G., White, R.N. & Gergely, P. 1991. Shake Table Test of a 1/8 Scale Three-Story Lightly Reinforced Concrete Building. *Technical Report NCEER-91-0018*. Buffalo: NCEER.

Feenstra, P.H., Rots, J.G., Arnesen, A., Teigen, J.G. & Hoiseth, K.V. 1998. A 3D constitutive model for concrete based on a co-rotational concept. In Rene de Borst et al. (ed.), *Proceedings of the Euro-C 1998 Conference on Computational Modeling of Concrete Structures*, Badgastein: Balkema.

Han, T.S. 2001. *Interface Modeling of Composite Material Degradation*. Ph.D. Dissertation, Cornell University.

Ortiz, M. & Pandolfi, A. 1999. Finite-deformation irreversible cohesive elements for three-dimensional crack-propagation analysis. *International Journal for Numerical Methods in Engineering* 44: 1267-1282.

Rots, J.G., Frissen, C.M. & Feenstra, P.H. 1999. Towards design rules based on snap-through analysis of composite concrete/masonry structures. In Avent, R.R. & Alawady, M. (ed.), *Structural Engineering in the 21st Century, Proc. 1999 Structures Congress*: 158-161. ASCE.

Shima, H., Chou, L. & Okamura, H. 1987. Micro and macro models for bond behavior in reinforced concrete. *Journal of the Faculty of Engineering, University of Tokyo (B)* 39(2): 133-194.

Shinozuka, M., Grigoriu, M., Ingraffea, A.R., Billington, S.L., Feenstra, P.H., Soong, T.T., Reinhorn, A.M. & Maragakis, E. 2000. Development of fragility information for structures and nonstructural components. *Research Progress and Accomplishments*: 15-32. Buffalo: MCEER.